Molecular Crystals and Liquid Crystals

Publication details, including instructions for authors and subscription information:
http://www.tandfonline.com/loi/gmcl20

3D Modelling of High Resolution Devices

Richard James [a], Mark C. Gardner [a], F. Aníbal Fernández [a] & Sally E. Day [a]

[a] Department of Electronic & Electrical Engineering, University College London, Torrington Place, London

Version of record first published: 31 Aug 2006

To cite this article: Richard James, Mark C. Gardner, F. Aníbal Fernández & Sally E. Day (2006): 3D Modelling of High Resolution Devices, Molecular Crystals and Liquid Crystals, 450:1, 105/[305]-118/[318]

To link to this article: http://dx.doi.org/10.1080/15421400600587860

Mol. Cryst. Liq. Cryst., Vol. 450, pp. 105/[305]–118/[318], 2006

ISSN: 1542-1406 print/1563-5287 online
DOI: 10.1080/15421400600587860

Taylor & Francis
Taylor & Francis Group

3D Modelling of High Resolution Devices

Richard James
Mark C. Gardner
F. Aníbal Fernández
Sally E. Day
Department of Electronic & Electrical Engineering, University College London, Torrington Place, London

An LCOS device has been simulated for both holographic and image display applications. A chequerboard pattern of on-off voltages has been applied in order to represent the highest supported spatial resolution. The accuracy with which this pattern is reproduced is presented as the pixel area is altered. It was found desirable to use a liquid crystal surface alignment conformal, as opposed to oblique, to the pixel grid in order to achieve sharp transitions between on and off pixels.

Keywords: 3D modeling; LCOS; liquid crystal devices; surface alignment

1. INTRODUCTION

Liquid crystals are increasingly used in a variety of applications such as beam steering, holographic storage and projection displays, where performance is limited by the available spatial resolution. For electrically addressed devices spatial resolution is determined by the pixel dimensions. Recently LCOS (liquid crystal on silicon) technology has provided an affordable and effective means to manufacture high resolution electrically addressed devices. There is a need for modelling in the initial design stages to avoid the expense of repeated redesign of the photo-mask. Three-dimensional modelling [1] is necessary to describe the defect structures that arise in real devices, and due to the rapid changes in the orientation of the liquid crystal, it is important to account for diffractive effects when calculating propagation of light [2].

The authors would like to acknowledge the support of EPSRC.

Address correspondence to Richard James, Department of Electronic and Electrical Engineering, University College London, Torrington Place, London, WC1E 7JE, UK. E-mail: r.james@ee.ucl.ac.uk

For applications such as holography and high definition television a very large number of pixels are required in order to achieve a large area of high resolution [3]. LCOS technology provides a means of delivering high resolution spatial modulation, with high manufacturing yield and cost effectiveness. However, fabrication limitations on the interpixel spacing mean that increasing the number of pixels on a given area leads to a smaller pixel size compared to the interpixel gap (reduced fill-factor). As the pixel size is reduced, the impact of LC disclinations increases so that disclinations can occupy a significant proportion of the device area.

We consider an LCOS configuration where the interpixel gap is fixed, while the electrode area is reduced. An alternating pattern of on-off voltages is applied to the pixel array to represent the highest spatial resolution that the system can support. From the calculated director orientation both the phase and intensity of the reflected light is determined. The implications for holographic and image display applications (in terms of the diffraction pattern and the modulation transfer function (MTF) respectively) will be presented.

2. COMPUTATIONAL METHOD

The modelling comprises two steps; the determination of the orientation of the liquid crystal molecules in response to the applied voltage, followed by the calculation of light propagation through this anisotropic medium. For three-dimensional analysis of the liquid crystal a method based on a variational approach to the Oseen-Frank free energy formulation has been developed [1]. The free energy, using three elastic constants and a vectorial description of the director field, where the director $\vec{n}$ is a representation of the average direction of the LC molecules integrated over a small volume, is given by:

$$F = \frac{1}{2}\int_{\Omega}\left\{\begin{array}{l} K_{11}(\nabla\cdot\vec{n})^2 + K_{22}(\vec{n}\cdot\nabla\times\vec{n}+q_o)^2 + K_{33}(\vec{n}\times\nabla\times\vec{n})^2 \\ -\epsilon_o[\Delta\epsilon(\vec{n}\cdot\vec{E})^2 + \epsilon_{\perp}(\vec{E}\cdot\vec{E})] \end{array}\right\} dV, \quad (1)$$

where K_{11}, K_{22}, and K_{33} are the elastic constants associated with splay, twist and bend deformations, q_o is the chirality of the LC, $\vec{E}$ is the electric field vector, ϵ_o is the permittivity of free space, $\Delta\epsilon$ is the dielectric anisotropy and $\epsilon_{\perp}$ is the permittivity perpendicular to the long axis of the molecule. The director relaxation equation can be derived from

$$\frac{\partial F}{\partial n_{\delta}} + \frac{\partial}{\partial \dot{n}_{\delta}}\left(\frac{\gamma}{2}\int_{\Omega}\dot{n}_{\mu}\dot{n}_{\mu}dV\right) = 0, \quad (2)$$

where γ is the rotational viscosity of the LC. This equation is discretised on a mesh of tetrahedral elements and is iterated until the steady state solution is obtained. Using a forward difference approximation for the time derivative leads to a matrix problem that can be written in the form:

$$\mathbf{G}\mathbf{n}^{\mathbf{t}+\delta\mathbf{t}} = \mathbf{W}\mathbf{n}^{\mathbf{t}}. \tag{3}$$

Solution of (3) for the director is alternated within each time step with the solution for the electric potential, based on the variational formulation:

$$\mathbf{J} = \int_{\Omega} \phi(\nabla \cdot \bar{\bar{\epsilon}} \cdot \nabla\phi) dV, \tag{4}$$

which upon discretisation using the same mesh of finite elements, leads to a matrix problem of the form:

$$\mathbf{A}\phi = 0. \tag{5}$$

Commonly the Jones [4] or Berreman [5] methods are used, in conjunction with ray-tracing techniques to determine the optical transmission of a liquid crystal cell. These methods do not take into account diffractive effects, and thus break down when there is rapid lateral variation of the director. There are several methods which take this effect into consideration, the finite-difference time-domain (FDTD) method, the beam propagation method and the coupled wave method [6]. In the coupled wave or grating method (GM) the cell is regarded as the fundamental unit of a periodic structure in the transverse plane, composed of several sublayers. Each sublayer has it own constant dielectric tensor. The electromagnetic field in each sublayer is decomposed into a sum of coupled plane waves, and so can be described by a transfer matrix A, which contains the transverse variation of the material properties. Maxwell's equations lead to an equation of the form:

$$\partial_z \psi = j k_o \mathbf{A} \psi, \tag{6}$$

where the vector ψ contains the transverse components of E and H in each layer. The propagation through all the layers can be found taking the product of these matrices. Due to the small pixel size, the order of the matrices is very large and the problem is computationally expensive. However, considerable savings are obtained by using a Lanczos procedure to reduce the order of the problem [2], and this approach has been taken for all optical calculations presented in this paper.

TABLE 1 Material Properties (E7)

K_{11}	K_{22}	K_{33}	$\epsilon_\perp$	$\Delta\epsilon$
11.1 pN	10.0 pN	17.1 pN	5.2	13.8

3. SIMULATION DETAILS

A nematic LCOS device with a pixelated reflector beneath an LC layer and a ground plane forms the basis of all simulations that follow. For both holographic and image display applications a pre-tilt of 2° is chosen to ensure consistent switching. The LC material chosen is Merck E7 and it's properties are listed in Table 1. Due to the differing wavelengths and modes of operation for each considered application, different applied voltages and cell thickness are required, which will be further detailed in the following sections. In order to test each device, the highest possible spatial resolution signal is applied, comprising a chequerboard pattern. A periodic modelling window, orientated at 45° to the pixel grid provides the minimum window area of $2 \times pitch^2$, where the pixel pitch refers to the pixel period including the interpixel gap which is held constant at 0.5 μm for all simulations.

4. DIFFRACTION DEVICE

There are numerous studies of 1D pixel arrays for holographic or beam steering applications [7–9], but these neglect the complex 3D defect structures that arise in real devices. In this paper an LCOS device for providing arbitrary phase modulation, using a 2D array of pixels is studied. The advantage in using a nematic LC is that analogue phase levels can be obtained. To achieve good performance without the need for a complex optical configuration, it is desirable to select a cell thickness that provides a phase excursion of 2π. To test the device, simulations have been performed while displaying the highest possible resolution; a 0 to 2π chequerboard in phase. This is the largest phase transition that will occur in a hologram, and it is important that this pattern can be accurately reproduced. Although a 2π chequerboard lacks practical application, it provides a simple means to quantify performance. Ideally a propagating wavefront would be unaffected by this phase modulation and power would be confined to the zero diffraction order. However the finite extent of LC deformations, and fringing fields between electrodes, blur the transitions in phase causing deflection into neighbouring diffraction orders.

Limited information on the material parameters of E7 is available at the near infrared wavelength of 1.55 μm that we are considering for this application, and so an extrapolated birefringence of $\Delta n = 0.189$ is used for the optical calculations. Using this birefringence, a device thickness in excess of 4.1 μm is required to give a 2π phase excursion when operating in the reflective mode.

A planar aligned cell, providing phase modulation, has been simulated and it is assumed that linearly polarised light is input to the device along the direction of the surface director. For telecommunications applications the device is required to be insensitive to the polarisation state of the incoming light. It is not the aim of this paper to address this issue, however placement of a quarter-wave plate (QWP) between the LC cell and the reflector can provide this insensitivity [9], but the doubling of phase excursion that is normally provided by the reflective mode is lost.

A potential difference that yields the required 2π phase excursion can be calculated for a given cell thickness by means of a 1D simulation. Normally the applied voltage is constrained by the driving circuitry, but it is advantageous both in terms of switching times, and minimizing the ratio of the thickness, d, to pixel pitch, to use as thin a cell as possible. A thin cell will require a higher driving voltage to achieve the same phase modulation as a thick cell. Two different cell thicknesses are studied; $d = 5\,\mu\text{m}$ with $3.04\,V$ applied, and $d = 4.5\,\mu\text{m}$ with 5.39 V applied.

Figure 1 shows the director and potential distribution at steady-state across a slice through the centre of the 5 μm thick LC cell. Two cases have been considered. Firstly a chequerboard voltage pattern was applied to the cell initially in the relaxed state, yielding the director profile shown in (a). Disclination formation is clearly visible at the centre of the righthand on-pixel, which causes deflection away from the zero diffraction order. Secondly a voltage bias of 1 V was applied to all electrodes prior to the chequerboard pattern, and the formation of a disclination is avoided. The resulting director profile is shown in (b).

From such director profiles the optical transmission can be calculated using the RGM, and because this is based on a spectral method, the diffraction pattern is directly available. Figure 2 shows the diffraction pattern for a pixel pitch of 21.2 μm. Diffraction into the higher diffraction orders occurs due to the finite extent of the on-off transitions, and this in turn results in a reduction in zero diffraction order.

Figure 3 shows the diffraction pattern yielded from 4.5 μm and 5.0 μm thick LC cavities, using alignment conformal to the pixel grid and a pixel pitch of 14.14 μm. A diagonal plot across the diffraction orders shown in Figure 2 has been made, and the resulting asymmetry

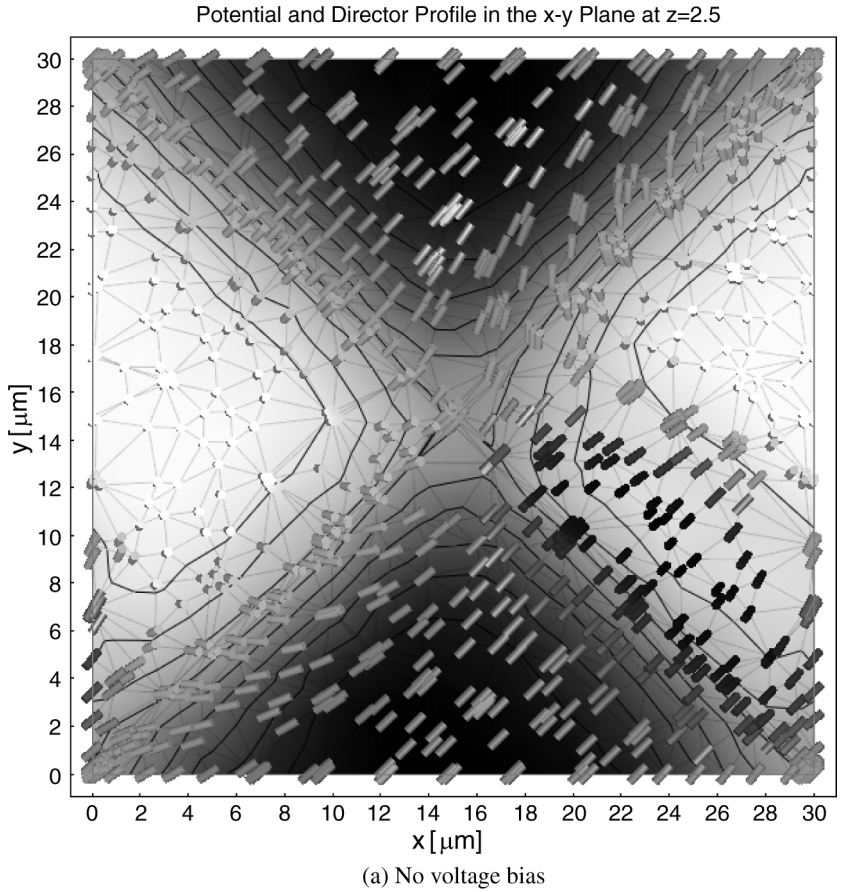

(a) No voltage bias

FIGURE 1 Director and potential distribution with a pixel pitch of 21.2 μm.

in the positive and negative orders is due to the pretilt at the alignment surfaces. The higher applied voltage associated with the 4.5 μm cell results in an increased transitional region between on and off pixels, and a fall in the zero diffraction order, despite the reduced cell thickness. An advantage of the 4.5 μm cell is a reduction in the +1 and −1 diffraction orders, but as we are concerned mainly with the zero order, the 5 μm device is used for the remainder of the simulations presented in this section.

Figure 4 shows the magnitude of the zero diffraction order as the pixel pitch is altered for two different alignments; conformal and oblique (at 45°) to the pixel grid. Although there are two possible

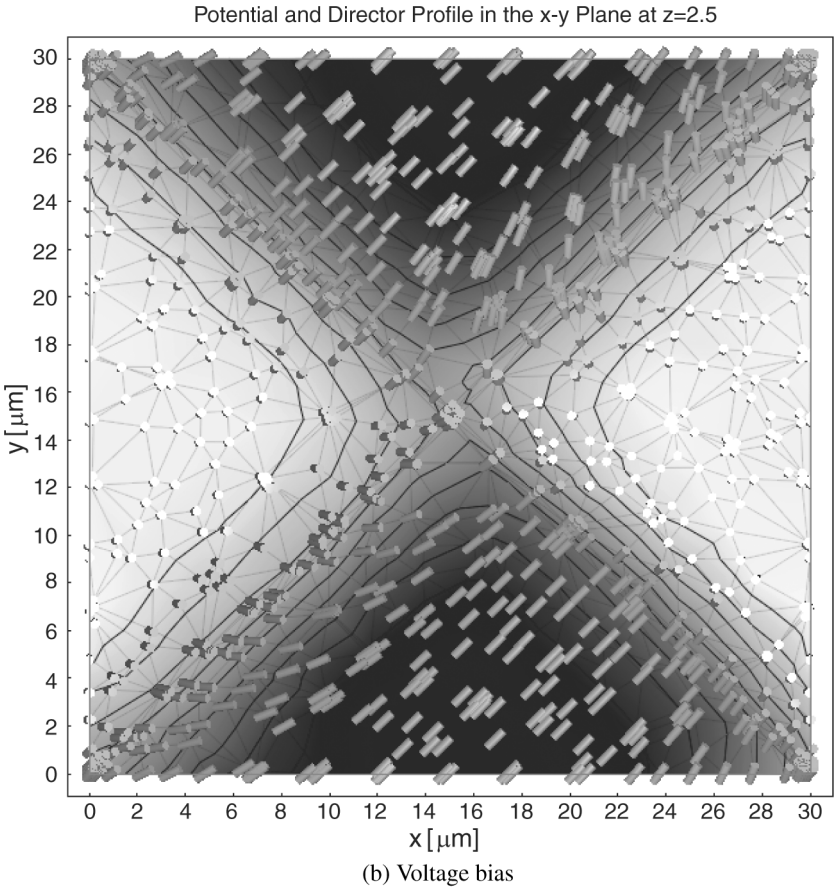

(b) Voltage bias

FIGURE 1 Continued.

conformal alignments, 0° and 90°, both were found to give identical results. Due to the disparate lengths of the interpixel gap and the pixel pitch, and the difficulties this poses for mesh generation, a limited maximum pitch of 35 μm has been simulated. Beyond this length, achieving a good quality mesh is difficult and the quantity of elements gives rise to a prohibitively large simulation time. When the pixel pitch is large in comparison to the cell thickness, interference between on-off pixels is low, and the 2π phase transitions are relatively abrupt. When the pixel pitch is decreased, the elastic deformation occupies a larger proportion of the device, leading to a decrease in both the phase excursion and the sharpness of the phase transitions, which results in

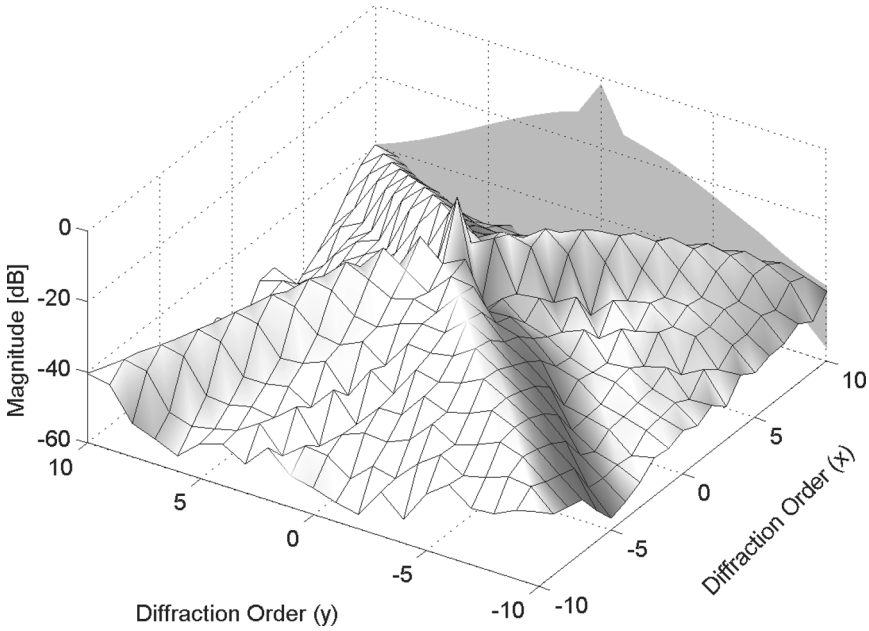

FIGURE 2 Diffraction pattern with a pixel pitch of 21.2 μm.

a decrease in the zero diffraction order. As the pixel pitch decreases further the device becomes incapable of describing the desired phase modulation and the zero diffraction order begins to rise as the device become ineffectual, as shown in the Figure 4 when the pixel pitch falls below 7 μm. Here the pixel pitch is of the same order as the cell thickness, and it is this large thickness that limits performance, not the size of the interpixel gap. When the alignment is oblique to the pixel grid, the angle between the director and the pixel edge is consistent across the whole device, and whilst this gives rise to symmetrical regions of twist within the LC, it results in inferior performance to conformal alignment, and the reason for this can be seen in Figure 1(b). Despite an increase in twist in comparison to the oblique case, only with conformal alignment is an abrupt change in the director seen across the electrode edges at the top-left and bottom-right of the figure.

5. IMAGE DISPLAY CONFIGURATION

The twisted nematic (TN) mode is widely used in active matrix liquid crystal displays, but in a reflective device this mode results in poor brightness and low resolution. A mixed-mode twisted nematic (MTN)

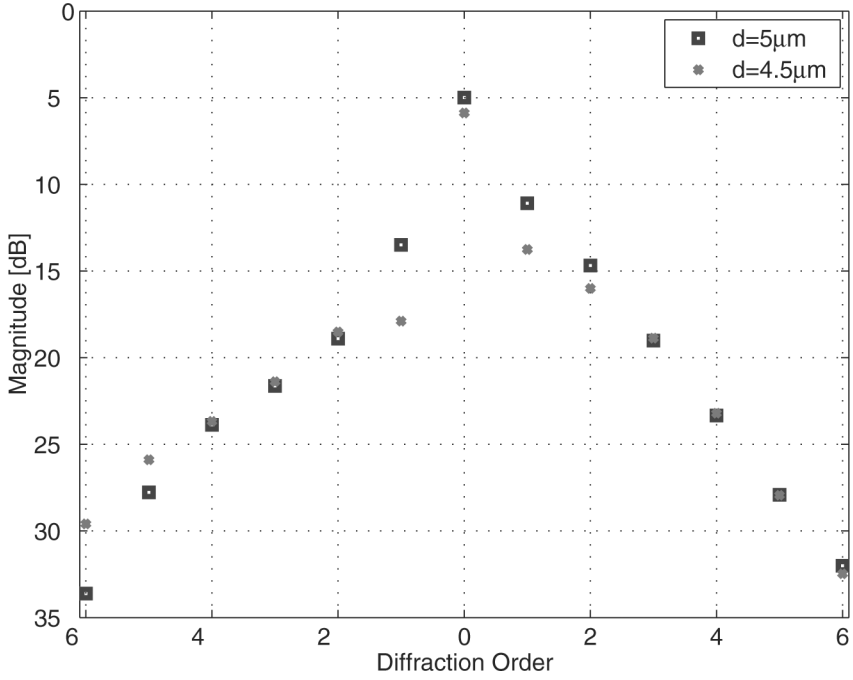

FIGURE 3 Diffraction pattern resulting from 4.5 μm and 5.0 μm thick LC cell with a pixel pitch of 14.14 μm.

[10] cell has been simulated which eliminates both of these problems. In the TN mode a thick LC cell guides the light through a 90° rotation, and the cell, which is placed between crossed polarisers, transmits light. When operated in the reflective mode, the necessary inclusion of an analyzer between the cell and mirror reduces the available brightness. Furthermore, the parallax limit on resolution caused by off-axis rays passing through adjacent pixels on forward and reflected paths is exacerbated by the finite thickness of the analyzer. The MTN cell has a smaller cell thickness and so only partial guiding of the light is performed by the 90° twist of the LC. The analyser between the LC cell and the reflector is omitted, and the combined guiding and birefringence effect can be fully exploited.

We consider a common reflective-mode projection system using a polarising beam splitter (PBS). The PBS directs light of one polarisation onto the LC device and selects the orthogonal polarisation reflected from the cell, thus acting as a pair of crossed polarisers. For practical and economic reasons, it is usual to rub the alignment

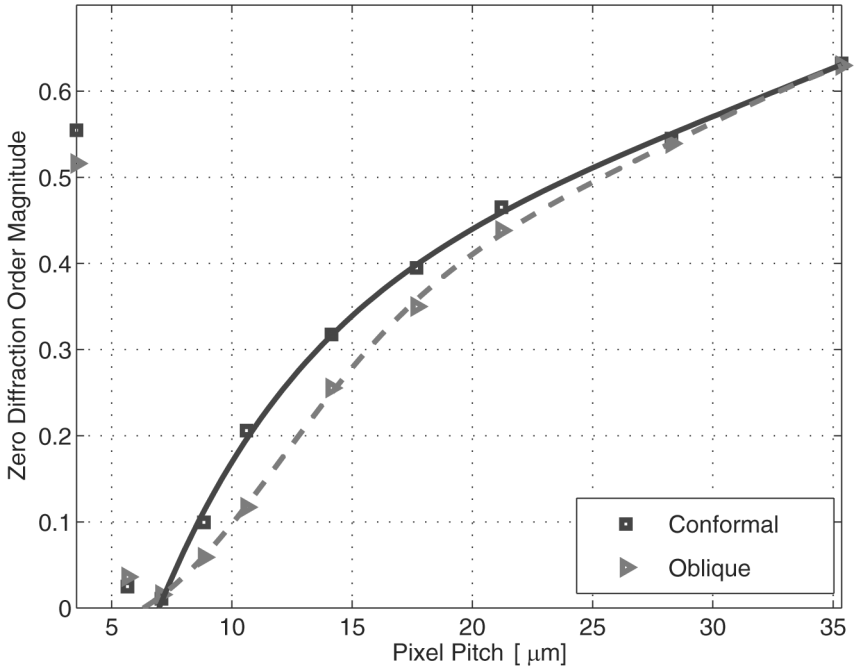

FIGURE 4 Effect of pixel pitch on 0 Diffraction order magnitude for alignments both conformal and oblique to the pixel grid.

layers at 20° and 110° to the pixel edges and have the PBS conformal with pixel edges rather than have conformal alignment and the PBS aligned at 20° to the pixel edges. As in the holographic application the pixel voltage is limited by the driving circuitry, but it is beneficial in terms of contrast ratio, to use as high a voltage as possible. Again we test the ability of the device to display the highest possible resolution, a chequerboard pattern, using applied voltages of 0 V and 5 V.

A single operation wavelength of $\lambda = 0.55\,\mu\text{m}$ has been considered, and at this wavelength the material exhibits a birefringence of $\Delta n = 0.2253$. The cell thickness for optimum contrast ratio is given by $d = 0.45\lambda/\Delta n$, where it is necessary to compensate for the effective reduction in birefringence caused by the pre-tilt. A cell thickness of 1.1 μm is required, and due to the reduced cross-sectional aspect ratio compared to the holographic application, sharper transitions between on and off pixels are achieved.

Figure 5 shows the optical reflectance of a device with a pixel pitch of 10.6 μm and an interpixel gap of 0.5 μm. At the centre of the figure, the interpixel gap is seen to occupy a significant proportion of the

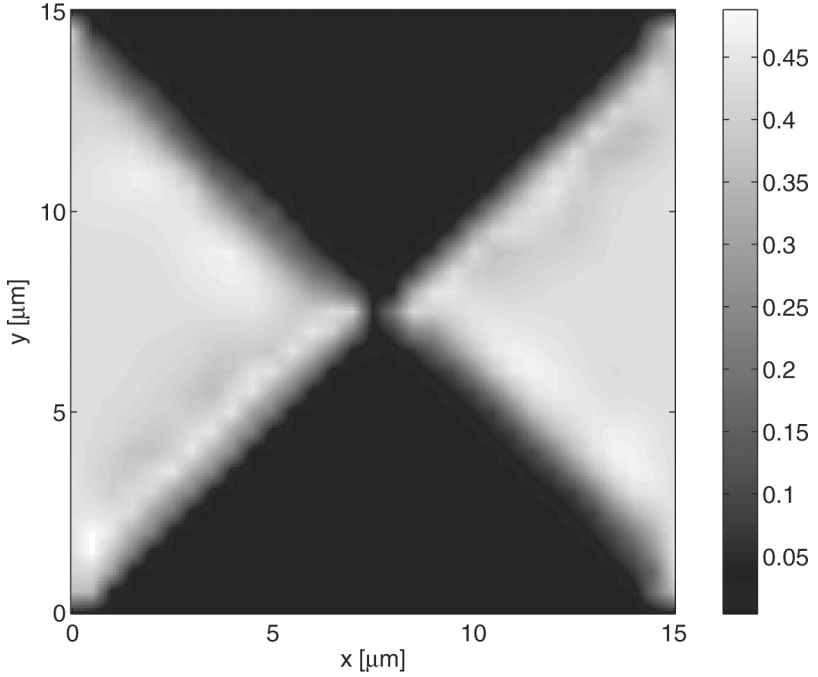

FIGURE 5 MTN cell reflectance for a pixel pitch of 10.6 μm.

device, but there is a rapid transition between the on and off regions due to the small cell thickness.

The modulation transfer function (MTF) is commonly used as a measure of the performance of lens systems and is defined as the modulation of the image divided by the modulation depth of the object [11]. If we work in terms of intensity, I, then the modulation can be defined as

$$M = \frac{I_{max} - I_{min}}{I_{max} + I_{min}}. \tag{7}$$

This definition is used when the stimulus is sinusoidal in nature, but for our purposes it is convenient to work in the frequency domain using a definition of the MTF in terms of the power spectrum density (PSD) of the image and the object [11]:

$$PSD_i(f) = MTF^2(f) PSD_o(f), \tag{8}$$

where the PSD can be calculated directly from the image as the square of the norm of the two dimensional Fourier transform.

The zero frequency component of the MTF indicates the mean reflectance over the area of interest, whereas the higher frequency components show the sharpness of the transition between bright and dark states. Figure 6 shows the zero and fundamental frequency components of the MTF as the pixel pitch is altered, and the interpixel gap is held constant. The object image chosen for the calculation of the MTF is that of an ideal chequerboard, neglecting the interpixel gap. Taking this gap into account would increase the MTF value for low pixel pitches, but would require an estimate of the reflectance within the gap. For small devices the interpixel gap takes up an increasing proportion of the device and the MTF reduces for all frequency components. If the LC layer is thicker than the interpixel gap, as is the case here, complete switching of the LC occurs as the pixel pitch approaches the size of this gap, and the displayed image becomes dark causing the MTF to drop to zero. It is the fundamental frequency that best measures the ability to display the highest resolution images, and this is seen to deteriorate as the pixel pitch falls below 6 μm.

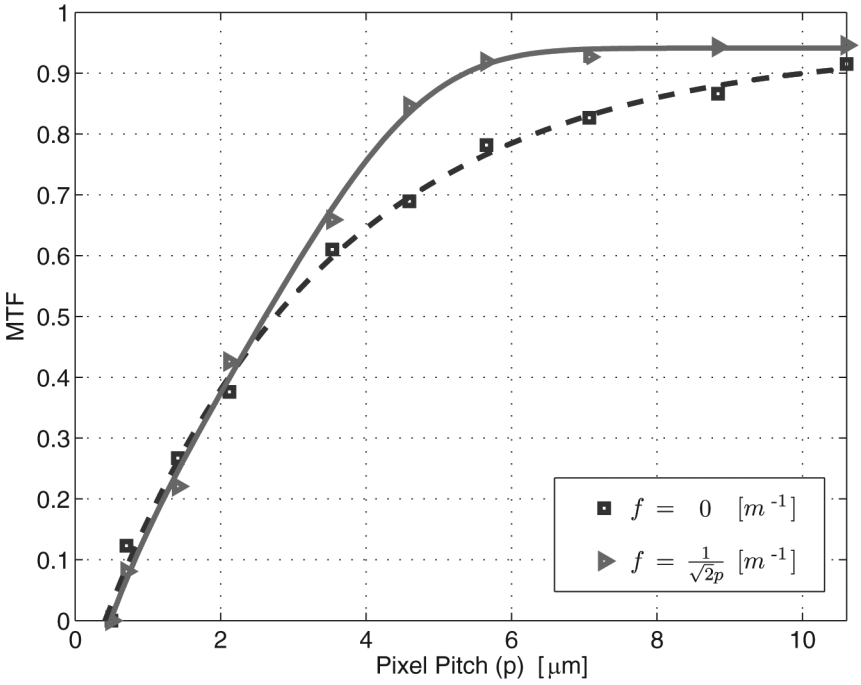

FIGURE 6 Modulation Transfer Function as a function of pixel pitch.

6. CONCLUSIONS

For the holographic application, precise control of potential difference is required to achieve a 2π phase difference between pixels. Any increase or decrease in voltage will alter this phase excursion and have a profound impact on the zero diffraction order magnitude. A thick LC cell is required and so fringing fields, which distort the liquid crystal, blur the phase transitions even when the pixel pitch is relatively large and the size of the interpixel gap is insignificant. The use of a nematic LC allows analogue phase levels to be achieved, and for a real applications the impact of a given pixel pitch to thickness ratio may be considerably less than for the 'worst case' examined here. In addition, the manufacture of high birefringence LC materials would allow a reduction in cell thickness, and marked improvement in performance. In the image display application maximising the voltage maximises the contrast ratio, and therefore maintains better operation as the pixel size diminishes compared to the holographic application. The MTN cell allows for a very thin LC cell and therefore sharp transitions occur between on and off pixels. Indeed, only as the pixel pitch is reduced below 6 μm does the fundamental frequency component of the MTN fall below 0.9, as the interpixel gap begins to occupy a significant proportion of the device.

REFERENCES

[1] Fernández, F. A., Day, S. E., Trwoga, P., Deng, H., & James, R. (March 2002). Three-dimensional dynamic modelling of liquid crystal display cells using finite elements. *Mol. Cryst. & Liq. Cryst.*, *375*, 291–299.

[2] Peverini, O. A., Olivero, D., Oldano, C., de Boer, D. K. G., Cortie, R., Orta, R., & Tascone, R. (September 2002). Reduced-order model technique for the analysis of anisotropic inhomogeneous media: Application to liquid-crystal displays. *J. Opt. Soc. Am. A*, *19*, 1901.

[3] Stanley, M. et al. (2004). 3D electronic holography display system using a 100-megapixel spatial light modulator. *Proceedings of the SPIE; Optical Design and Engineering*, *5249*, 297–308.

[4] Jones, R. C. (1941). A new calculus for the treatment of optical systems - I. Description and discussion of the calculus. *J. Opt. Soc. Am.*, *375*, 488–493.

[5] Berreman, D. W. (1972). Optics in stratified and anisotropic media: 4^* 4-matrix formulation. *J. Opt. Soc. Am.*, *62*, 502–510.

[6] Rokushima, K. & Yamakita, J. (1983). Analysis of anisotropic dielectric gratings. *J. Opt. Soc. Am.*, *73*, 901–908.

[7] McManamon, P. F., Watson, E. A., Dorschner, T. A., & Barnes, L. J. (1993). Applications look at the use of liquid crystal writable gratings for steering passive radiation. *Opt. Eng.*, *32*, 2657–2664.

[8] Brown, C. V., Kriezis, Em. E., & Elston, S. J. (2002). Optical diffraction from a liquid crystal phase grating. *J. Appl. Phys.*, *91*, 3495–3500.

[9] Komarcevic, M., Manolis, I. G., Wilkinson, T. D., & Crossland, W. A. (2005). Polarization effects in reconfigurable liquid crystal phase holograms. *Opt. Commun.*, *244*, 105–110.
[10] S.-T. Wu & C.-S. Wu. (March 1996). Mixed-mode twisted nematic liquid crystal cells for reflective displays. *Applied Physics Letters*, *68*(11), 1455–1457.
[11] Levy, E., Peles, D., Opher-Lipson, M., & Lipson, S. G. (February 1999). Modulation transfer function of a lens measured with a random target method. *Applied Optics*, *38*, 679.